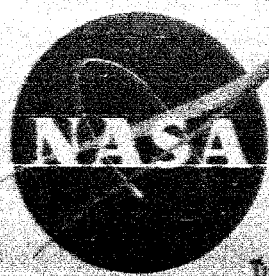


NASA TM X-594

NOT SUBJECT TO AUTOMATIC CLASSIFICATION CHANGE NASA ORDER 41-5-1



REMOVED FROM CATEGORY 7 AUTHORITY- MEMO FROM DROBKA TO LEBOW DATED 4/23/66

JUN - 9 1966

Declassified by authority of NASA Classification Change Notices No. 47 Dated **4/23/66

TECHNICAL MEMORANDUM

X-594

DECLASSIFIED- AUTHORITY US: 12885 DROBKA TO LEBOW MEMO DATED 6/8/66

TRANSONIC WIND-TUNNEL MEASUREMENTS OF SOME DYNAMIC LONGITUDINAL AND DIRECTIONAL STABILITY PARAMETERS FOR A FINNED SPINNING BODY OF REVOLUTION HAVING A HIGH FINENESS RATIO

By William C. Hayes, Jr., and Robert A. Kilg

Langley Research Center Langley Air Force Base, Va.

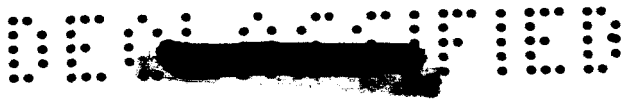
N66 33323
ACCESSION NUMBER
20
(PAGES)
X-594
NASA OR OTHER AGENCY REPORT

7
01
CATEGORY

GPO PRICE \$
CFSTI PRICE(S) \$
Hard copy (HC)
Microfiche (MF)

NATIONAL AERONAUTICS AND SPACE ADMINISTRATION
WASHINGTON
October 1961

B



NATIONAL AERONAUTICS AND SPACE ADMINISTRATION

TECHNICAL MEMORANDUM X-594

TRANSONIC WIND-TUNNEL MEASUREMENTS OF SOME DYNAMIC
LONGITUDINAL AND DIRECTIONAL STABILITY PARAMETERS

FOR A FINNED SPINNING BODY OF REVOLUTION

HAVING A HIGH FINENESS RATIO*

By William C. Hayes, Jr., and Robert A. Kilgore

SUMMARY

33323

Forced-oscillation tests were made at Mach numbers between 0.60 and 1.20 to determine the damping in pitch and in yaw and the oscillatory longitudinal and directional stability parameters of a finned body of revolution of high fineness ratio free to spin about the longitudinal axis. The mean angle of attack generally varied from -4° to 12° , the reduced-frequency parameter from 0.0020 to 0.0192, and the spin rate from 109 to 226 radians per second. The results of the tests showed that a 40-percent increase in the basic tail-fin area increased the damping in pitch and provided a longitudinally stable configuration. This configuration also had positive damping in yaw and directional stability.

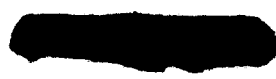
Author

INTRODUCTION

Missiles are often designed to spin about the longitudinal axis in order to alleviate the adverse effects of asymmetry or thrust misalignment. However, as a result of the coupling of the gyroscopic torque due to spin and the aerodynamic torque due to angle of attack, a precessional type of motion can result with possible adverse effects on range and accuracy. See, for example, reference 1. In order to alleviate these effects it is necessary, therefore, that any planar motion, such as that initiated by turbulence, be damped before large precessional motion can become established.

The purpose of the present investigation was to determine some of the dynamic longitudinal and directional stability characteristics of a

*Title, Unclassified.



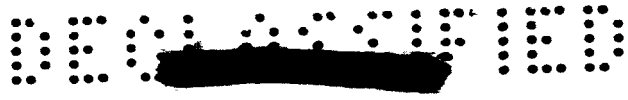


body of revolution subjected to aerodynamically induced spin about the longitudinal axis. The model, which had an ogival nose and a fineness ratio of 11.57, was tested with fins off and with two tail-fin configurations. The dynamic longitudinal and directional stability parameters were determined and are presented as functions of angle of attack. Tests were made at Reynolds numbers from 0.86×10^6 to 1.14×10^6 corresponding to a Mach number range from 0.60 to 1.20. The reduced-frequency parameter varied from 0.0020 to 0.0192 and the spin rate varied from 109 to 226 radians per second. The angle-of-attack range for most pitch tests was from -4° to 12° and the angle-of-attack range for the yaw tests was from 0° to 10° .

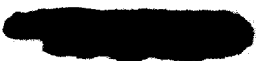
SYMBOLS

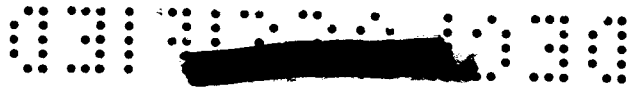
The data are presented relative to the body-axis system. The origin of the axis system is coincident with the center of oscillation located 63.83 percent of the body length rearward of the nose. The symbols used are defined as follows:

d	reference length, cylindrical diameter of the model, 0.271 ft
M	free-stream Mach number
p	spin rate, $\frac{\partial \phi}{\partial t}$, radians/sec
q	pitching velocity, $\frac{\partial \theta}{\partial t}$, radians/sec
q̇	pitching acceleration, $\frac{\partial^2 \theta}{\partial t^2}$, radians/sec ²
r	yawing velocity, $\frac{\partial \psi}{\partial t}$, radians/sec
ṙ	yawing acceleration, $\frac{\partial^2 \psi}{\partial t^2}$, radians/sec ²
R	Reynolds number
S	reference area, $\frac{\pi d^2}{4}$, 0.0576 sq ft
t	time, sec



- V free-stream velocity, ft/sec
- α instantaneous angle of attack, radians
- α_0 mean angle of attack, deg
- $\dot{\alpha}$ time rate of change of angle of attack, $\frac{\partial \alpha}{\partial t}$, radians/sec
- β instantaneous angle of sideslip, $\sin \beta = -\sin \psi \cos \alpha$, radians
- $\dot{\beta}$ time rate of change of angle of sideslip, $\frac{\partial \beta}{\partial t}$, radians/sec
- ϕ instantaneous angle of roll, radians
- θ instantaneous angle of pitch, radians
- ρ free-stream mass density of air, $\frac{\text{lb-sec}^2}{\text{ft}^4}$
- ψ instantaneous angle of yaw, radians
- ω angular velocity, 2π (Frequency of oscillation), radians/sec
- $\frac{\omega d}{V}$ reduced-frequency parameter, radians
- C_m pitching-moment coefficient, $\frac{\text{Pitching moment}}{\frac{\rho V^2 S d}{2}}$
- C_n yawing-moment coefficient, $\frac{\text{Yawing moment}}{\frac{\rho V^2 S d}{2}}$
- $C_{m\alpha} = \frac{\partial C_m}{\partial \alpha}$ per radian
- $C_{n\beta} = \frac{\partial C_n}{\partial \beta}$ per radian
- $C_{mq} = \frac{\partial C_m}{\partial \left(\frac{qd}{V}\right)}$ per radian





$$C_{m\dot{\alpha}} = \frac{\partial C_m}{\partial \left(\frac{\dot{\alpha}d}{V}\right)} \text{ per radian}$$

$$C_{n_r} = \frac{\partial C_n}{\partial \left(\frac{rd}{V}\right)} \text{ per radian}$$

$$C_{n\dot{\beta}} = \frac{\partial C_n}{\partial \left(\frac{\dot{\beta}d}{V}\right)} \text{ per radian}$$

$$C_{m\dot{q}} = \frac{\partial C_m}{\partial \left(\frac{\dot{q}d^2}{V^2}\right)} \text{ per radian}$$

$$C_{n_r\dot{r}} = \frac{\partial C_n}{\partial \left(\frac{\dot{r}d^2}{V^2}\right)} \text{ per radian}$$

$C_{m_q} + C_{m\dot{\alpha}}$ damping-in-pitch parameter, per radian

$C_{n_r} - C_{n\dot{\beta}} \cos \alpha_0$ damping-in-yaw parameter, per radian

$C_{m\alpha} - \left(\frac{\omega d}{V}\right)^2 C_{m\dot{q}}$ oscillatory longitudinal stability parameter,
per radian

$C_{n\beta} \cos \alpha_0 + \left(\frac{\omega d}{V}\right)^2 C_{n_r\dot{r}}$ oscillatory directional stability parameter,
per radian

APPARATUS AND MODEL

These tests were made in the Langley 8-foot transonic pressure tunnel using the sting-mounted forced-oscillation mechanism described in reference 2. Dimensions of the model, which was constructed of magnesium, are presented in figure 1. The basic model was a body of revolution having a fineness ratio of 11.75, an ogive nose, and a cylindrical afterbody. Canted tail fins mounted on the afterbody produced the desired spin rate by using differential deflections of 1° and 3° on alternate pairs of diametrically opposed fins. The model was designed so that the tail-fin area could be increased by about 40 percent by the addition of fin-extension panels.



The model was mounted on specially designed high-precision bearings which allowed the model to spin about its longitudinal axis. The bearings were mounted on a shaft which was attached to the oscillating moment balance so that the model was forced to oscillate in pitch or yaw while free to spin. Wind-off tests indicated spin rate had no measurable effect on the contribution of the bearing assembly to pitch or yaw damping moment. Changes in rolling friction due to load do not affect damping measured in the pitch or yaw plane. The spin rate was measured by an internally mounted induction coil pick up and pulse generator which provided a signal for an electronic counter. A diagram of the model and internally mounted equipment is shown in figure 2.

All tests were made with three-dimensional roughness consisting of number 60 carborundum particles applied in a band around the model nose as shown in figure 1.

PROCEDURE AND TESTS

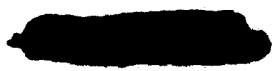
The model was forced to perform either a pitching or yawing oscillation of about 2° amplitude while measurements of the torque required to produce the known oscillation were obtained. A detailed discussion of the principles of measuring dynamic stability with this forced-oscillation technique is presented in appendix A of reference 3.

Tests were made at a tunnel stagnation pressure of 1 atmosphere for Mach numbers of 0.60, 0.80, 1.00, and 1.20 with the corresponding Reynolds numbers based on the cylindrical diameter of the model varying from 0.86×10^6 to 1.14×10^6 as shown in figure 3. The mean angle of attack α_0 varied from -4° to 12° for most pitch-oscillation tests and α_0 varied from 0° to 10° for the yaw-oscillation tests. The reduced-frequency parameter $\omega d/V$ varied from 0.0020 to 0.0192 and the spin rate varied from 109 to 226 radians per second.

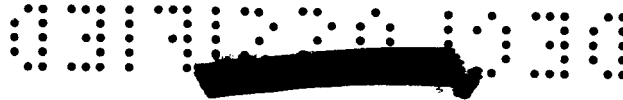
Wind-off values used in the data reduction process were obtained with the model in a nonspinning condition so that the wind-on data as presented include the contribution of the aerodynamically induced spinning on the dynamic stability parameters.

RESULTS AND DISCUSSION

The damping and oscillatory stability parameters are presented as functions of α_0 for each of the test Mach numbers in figures 4 to 7.



L
1
6
2
8



Tests of the nonspinning body alone (fins off) in the lower range of reduced-frequency parameter $\left(\frac{\omega d}{V} = 0.0020 \text{ to } 0.0037\right)$ indicated large aperiodic excursions of the damping-in-pitch parameter $C_{m\dot{\alpha}} + C_{m\dot{\alpha}}$ at a constant α_0 and Mach number as shown by the unflagged symbols in figure 4. Inasmuch as the presence of these excursions was well defined, data points were obtained near the limits of the excursions whenever they occurred. The extreme variations of damping in pitch, including reversals of sign, are probably associated with a flow separation and reattachment phenomenon which occurred intermittently during the low-frequency oscillation tests. Tests of the same configuration at a higher range of reduced-frequency parameter $\left(\frac{\omega d}{V} = 0.0092 \text{ to } 0.0192; \text{ flagged symbols}\right)$ did not produce any similar excursions in the damping in pitch for a given set of test conditions. The positive values of the oscillatory longitudinal stability parameter $C_{m\alpha} - \left(\frac{\omega d}{V}\right)^2 C_{m\dot{\alpha}}$, which indicate instability, show general agreement with the subsonic results for a similar model presented in reference 4.

The installation of the basic fins induced a spin rate which varied but slightly with α_0 within the ranges defined in figure 5. This configuration exhibited positive damping in pitch which generally increased with increasing α_0 . Although installation of the basic fins provided a large stabilizing increment in the oscillatory longitudinal stability parameter, this finned configuration remained longitudinally unstable.

An increase in fin area of about 40 percent, resulting from the attachment of the fin-extension panels to the basic fins, increased the damping in pitch and provided a longitudinally stable configuration at all test conditions. (See fig. 6.)

The damping in yaw and the directional stability parameters are presented for the extended-fins configuration in figure 7. No attempt has been made to evaluate the contribution to these parameters arising from magnus forces inasmuch as at the relatively low values of α_0 and spin rate of these tests they are expected to be small. This configuration exhibited positive damping in yaw and oscillatory directional stability for all test conditions.

CONCLUDING REMARKS

Wind-tunnel tests were made to determine the damping in pitch, damping in yaw, oscillatory longitudinal stability, and oscillatory directional stability at transonic speeds of a finned spinning body



DECLASSIFIED

7

having a high fineness ratio. The results of the tests showed that a 40-percent increase in the basic tail-fin area increased the damping in pitch and provided a longitudinally stable configuration. This configuration also had positive damping in yaw and directional stability.

Langley Research Center,
National Aeronautics and Space Administration,
Langley Field, Va., June 27, 1961.

REFERENCES

1. Bird, John D., and Lichtenstein, Jacob H.: An Investigation of a Source of Short-Round Behavior of Mortar Shells. NACA RM L56G20a, 1956.
2. Bielat, Ralph P., and Wiley, Harleth G.: Dynamic Longitudinal and Directional Stability Derivatives for a 45° Sweptback-Wing Airplane Model at Transonic Speeds. NASA TM X-39, 1959.
3. Braslow, Albert L., Wiley, Harleth G., and Lee, Cullen Q.: Dynamic Directional Stability Derivatives for a 45° Swept-Wing—Vertical-Tail Airplane Model at Transonic Speeds and Angles of Attack, With a Description of the Mechanism and Instrumentation Employed. NACA RM L58A28, 1958.
4. Polhamus, Edward C.: Effect of Nose Shape on Subsonic Aerodynamic Characteristics of a Body of Revolution Having a Fineness Ratio of 10.94. NACA RM L57F25, 1957.

DECLASSIFIED

L
1
6
2
8

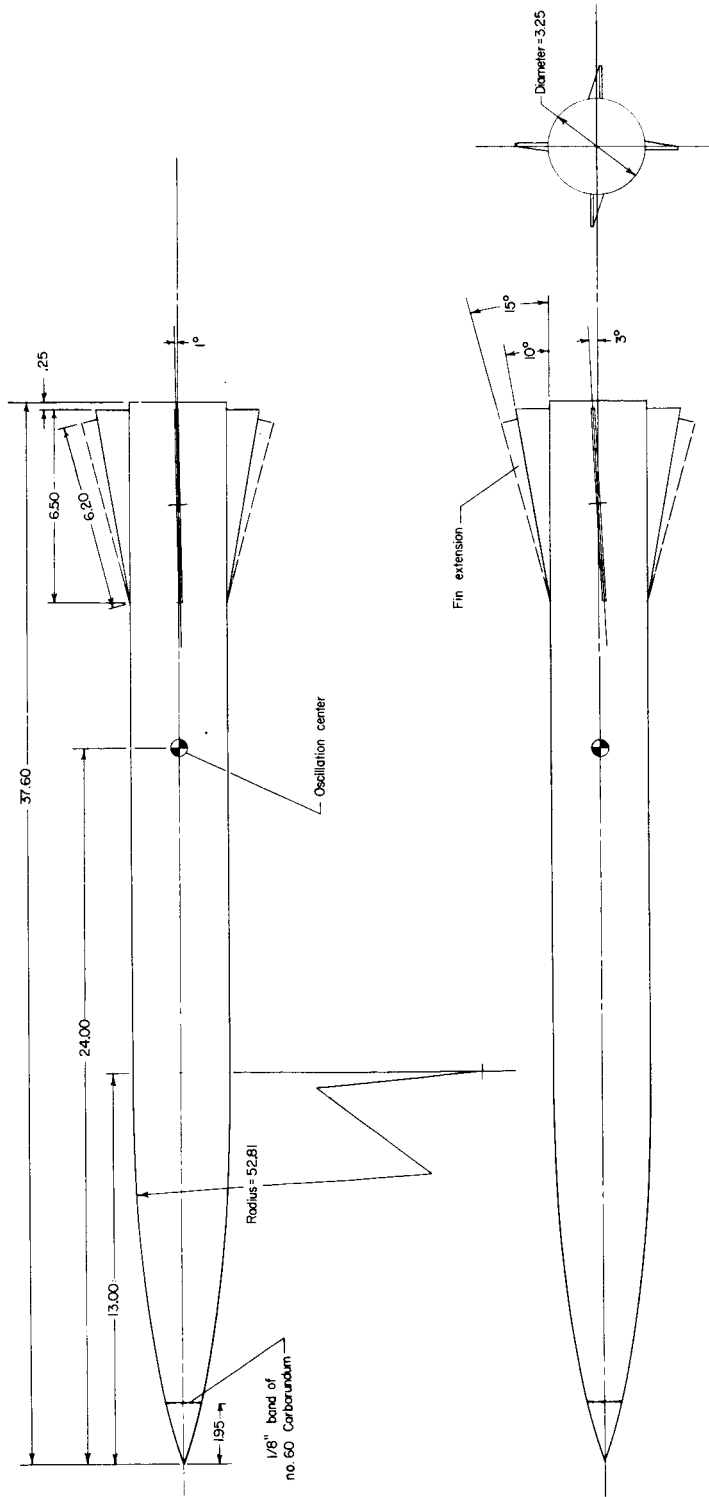


Figure 1.- Drawing of model. All linear dimensions are in inches. Maximum projected side area of basic fin is about 7 percent of the body projected side area. Maximum projected side area of fin and fin extension is about 10 percent of the body projected side area.

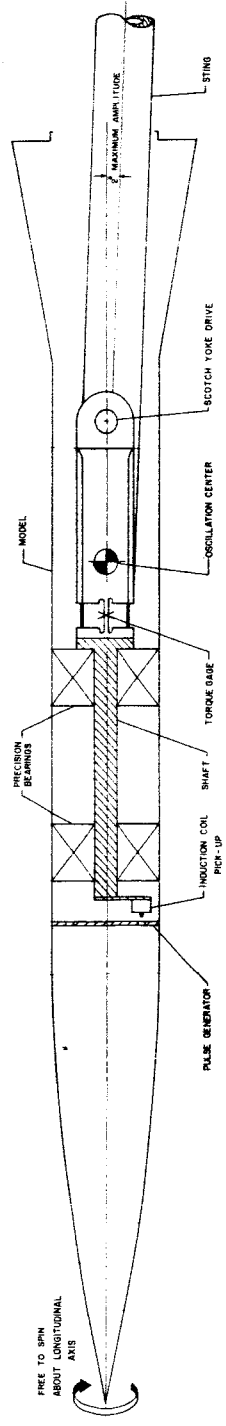
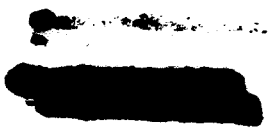


Figure 2.- Schematic diagram of rolling model mounted on forced-oscillation apparatus.



SECRET

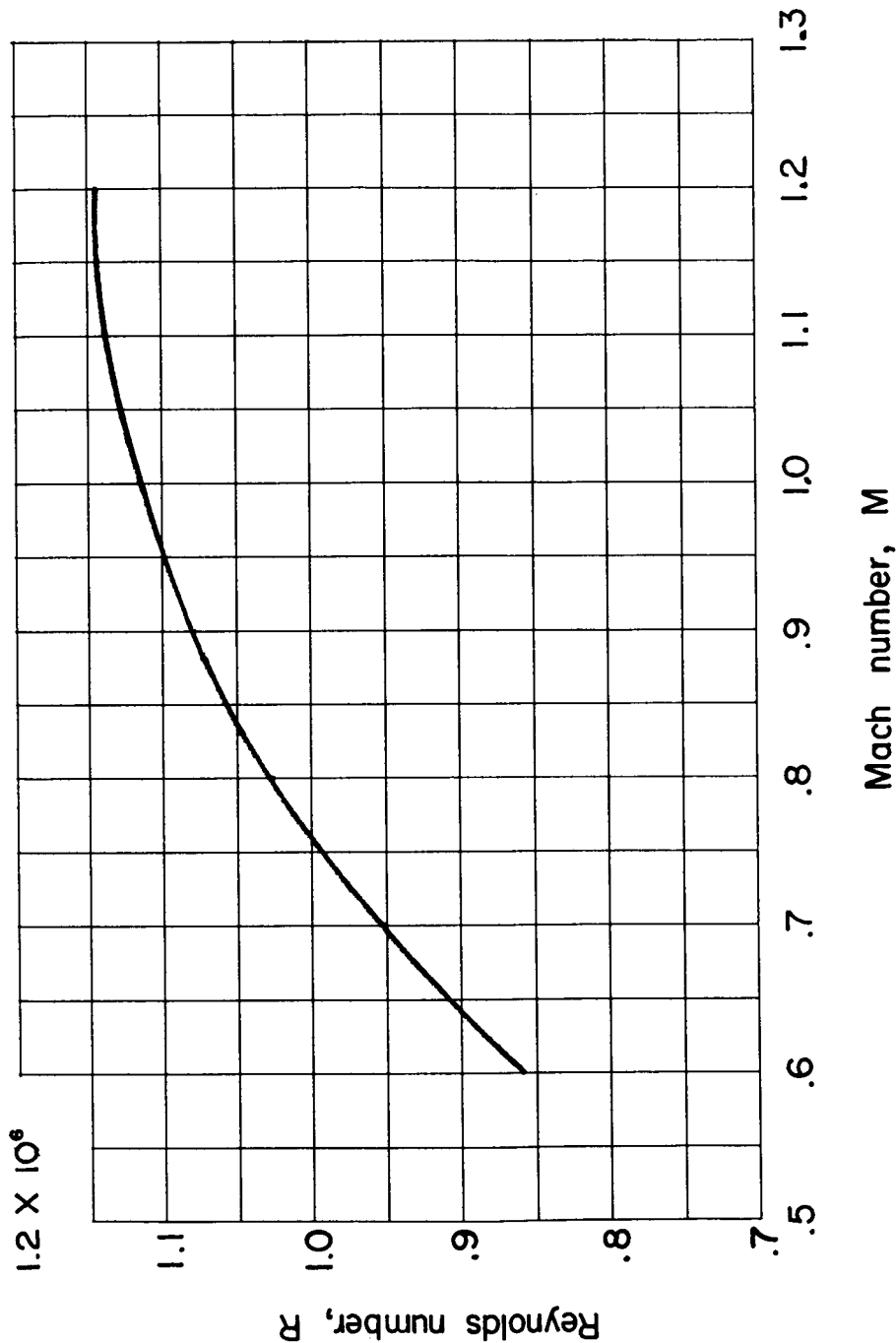


Figure 3.- Variation of Reynolds number with Mach number.

SECRET

L-1628

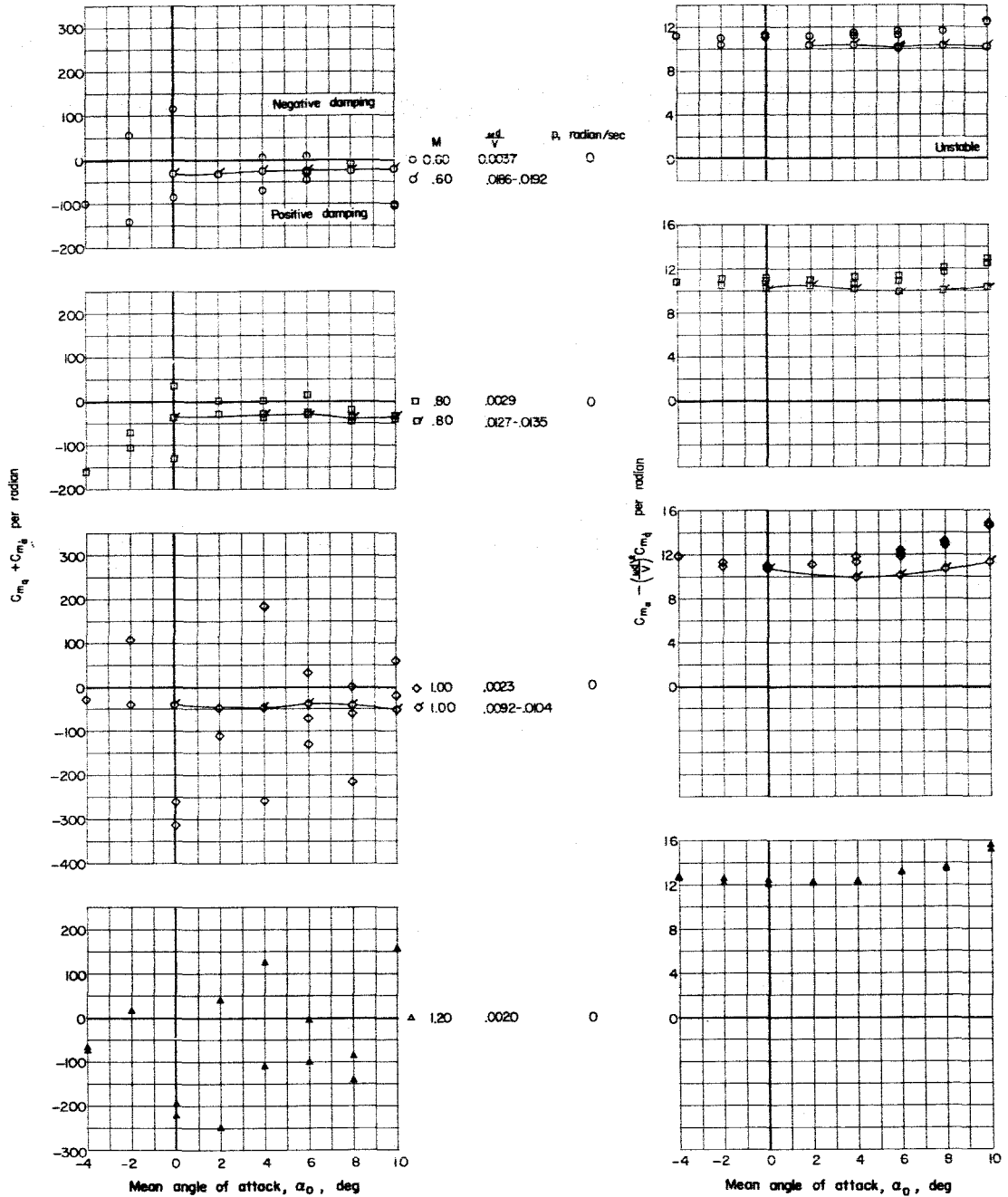


Figure 4.- Variation of damping-in-pitch parameter $C_{m_q} + C_{m_{\dot{\alpha}}}$ and oscillatory longitudinal stability parameter $C_{m_{\alpha}} - \left(\frac{\omega d}{V}\right)^2 C_{m_q}$ with mean angle of attack. Body alone.

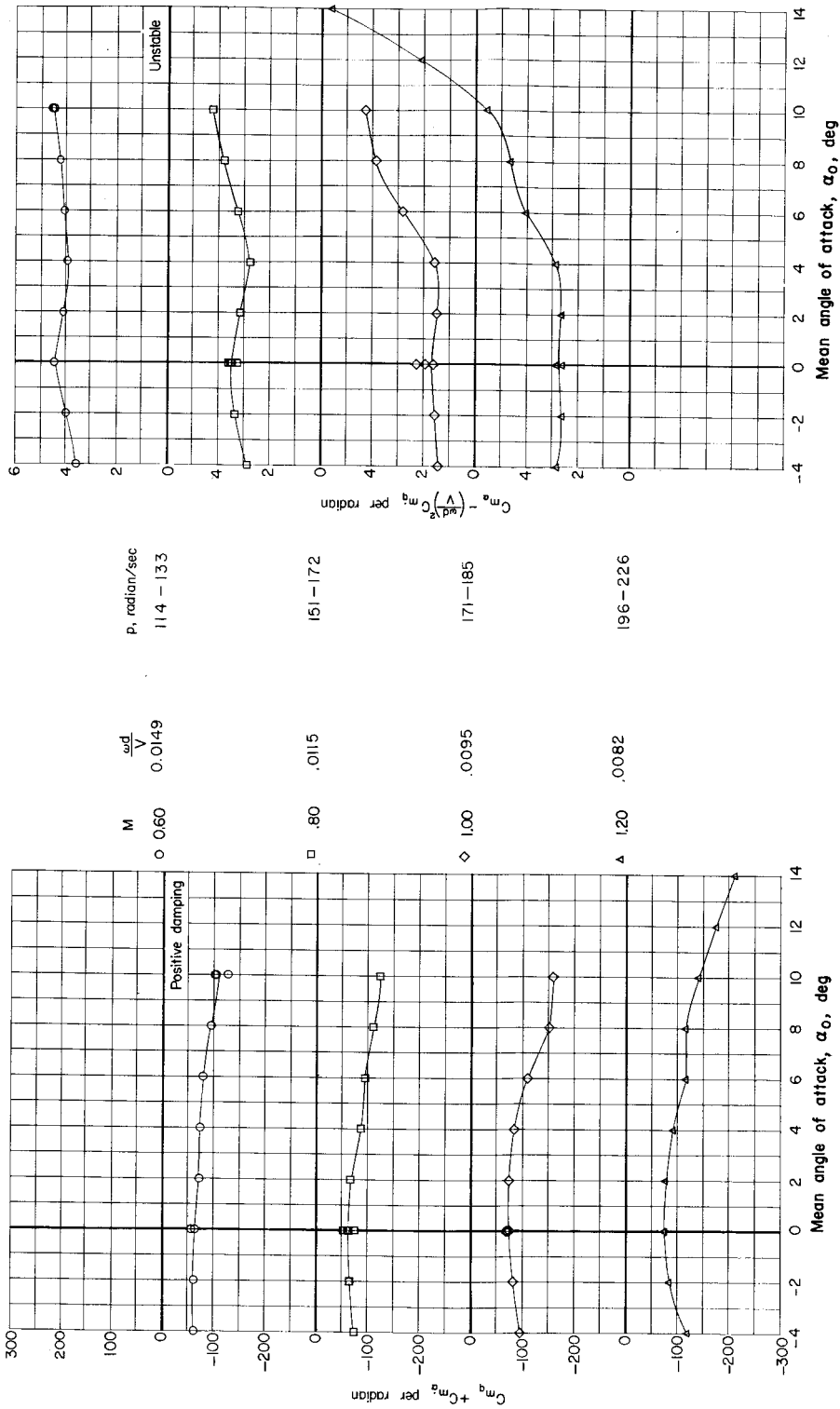
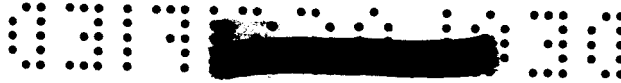


Figure 5.- Variation of damping-in-pitch parameter $C_{m_q} + C_{m_{\dot{\alpha}}}$ and oscillatory longitudinal stability parameter $C_{m_{\alpha}} - \left(\frac{\omega d}{V}\right)^2 C_{m_q}$ with mean angle of attack. Body plus basic fins.

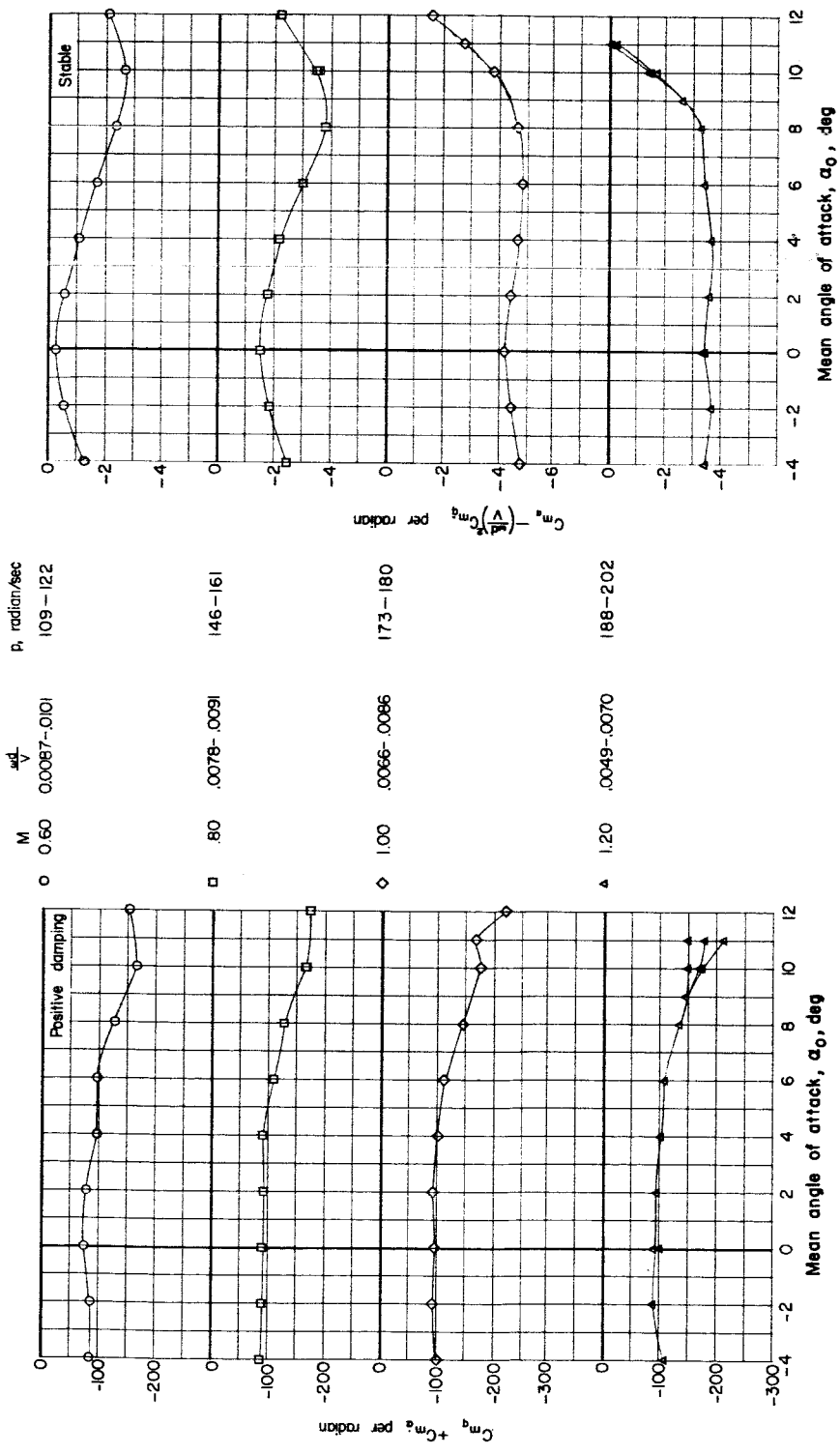


Figure 6. - Variation of damping-in-pitch parameter $C_{m\dot{\alpha}} + C_{m\ddot{\alpha}}$ and oscillatory longitudinal stability parameter $C_{m\ddot{\alpha}} - \left(\frac{u\dot{q}}{V}\right)^2 C_{m\dot{\alpha}}$ with mean angle of attack. Body plus fins with extensions.

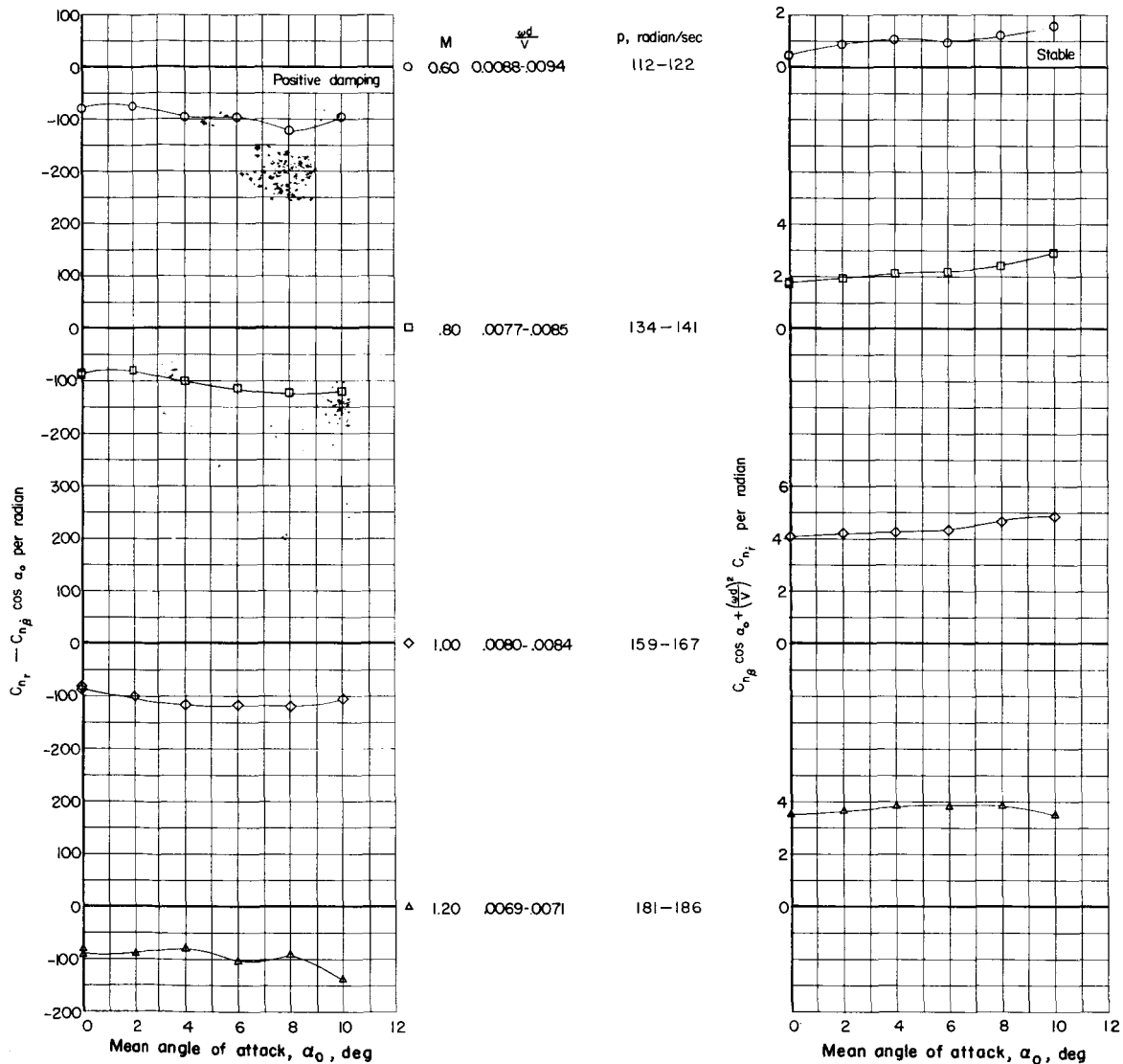
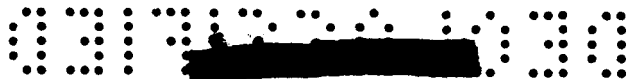


Figure 7.- Variation of damping-in-yaw parameter $C_{n_r} - C_{n_\beta} \cos \alpha_0$ and oscillatory directional stability parameter $C_{n_\beta} \cos \alpha_0 + \left(\frac{\alpha d}{V}\right)^2 C_{n_r}$ with mean angle of attack. Body plus fins with extensions.

L-1628